JCTC Journal of Chemical Theory and Computation

ARTICLE

pubs.acs.org/JCTC

Polarized Molecular Orbital Model Chemistry. 2. The PMO Method

Peng Zhang, Luke Fiedler, Hannah R. Leverentz, Donald G. Truhlar,* and Jiali Gao*

Department of Chemistry and Supercomputing Institute, University of Minnesota, 207 Pleasant Street S.E., Minneapolis, Minnesota 55455-0431, United States

Supporting Information

ABSTRACT: We present a new semiempirical molecular orbital method based on neglect of diatomic differential overlap. This method differs from previous NDDO-based methods in that we include p orbitals on hydrogen atoms to provide a more realistic modeling of polarizability. As in AM1-D and PM3-D, we also include damped dispersion. The formalism is based on the original MNDO one, but in the process of parametrization we make some specific changes to some of the functional forms. The present article is a demonstration of the capability of the new approach, and it presents a successful parametrization for compounds composed only of hydrogen and oxygen atoms, including the important case of water clusters.

1. INTRODUCTION

Molecular modeling methods for calculating potential energy surfaces and forces span a wide spectrum of accuracy and cost, ranging from pairwise potentials in molecular mechanics on the one hand to coupled cluster theory at the complete basis set limit on the other. But there is a large gap in computational cost between using semiempirical molecular orbital methods at the high end of the low end and small-basis-set Hartree−Fock or density functional theory at the low end of the high end. The goal of this work is to develop a new method in that gap, which can be applied to the study of the internal energies of a single molecule or a group of molecules and to macromolecular systems, including solvated proteins. In particular, we seek a method that is almost as inexpensive as the popular AM1[1] and PM3[2] semiempirical methods (both based on neglect of diatomic differential overlap[3,4] (NDDO)) but is more accurate in two key respects: (1) it gives more accurate noncovalent interactions, and (2) it yields more accurate molecular polarizabilities. Such a method would be well suited for use in the Explicit Polarization[5,6] (X-Pol) force field or in any simulation where it is important to include polarization and induction effects in a large system that requires extensive sampling of fluctuations or conformational states.

Our starting point is the MNDO[4] formalism, which has been the basis for the later, more successful AM1 and PM3 through PM6 series of model chemistries. It has the advantage as a starting point for new work in the treatment of effective nuclear core−core interactions. To this end, we make three key enhancements to MNDO:

- A set of p-type basis functions is added on the hydrogen atoms. The motivation for this is provided in the previous paper,[7] and we also note (i) the work of Parkinson and Zerner,[8] adding p functions on hydrogen to the INDO model chemistry to improve the calculation of hyperpolarizabilities and (ii) the SINDO1 and MSINDO methods of Jug and Bredow in which the basis can be augmented with p functions, where the motivation was a better treatment of hydrogen bonding.[9]
- A damped dispersion function is included as in the PM3-D method of Hillier and co-workers.[10−12]
- The new approximate molecular orbital method is parametrized against molecular polarizabilities and noncovalent interactions as well as static molecular data.

Since explicit p-type polarization functions on hydrogen atoms are incorporated into our method, it is called the polarized molecular orbital (PMO) model. We envision developing a new-generation semiempirical model that can be applied equally well both to the study of the internal energies of a single molecule or cluster of molecules and to dynamical simulation and modeling of condensed-phase systems, including liquids, liquid-phase solutions, and biological macromolecular interactions. Since water is essential for applications to all biomolecular interactions and to many other chemical systems, we first focus on the development of a model for compounds composed of hydrogen and oxygen that can be used as a basic starting point to create a balanced PMO model for describing intermolecular interactions. In particular, in the present article, we present the key theoretical ingredients, parametrization strategies, and computational details of PMO by parametrizing it for molecules composed of only O and H atoms. In this process, we make some changes in the functional forms used for fitting electronic integrals in MNDO, but we consider these parametrization choices, not essential parts of the method. In principle, they could be changed in the future to develop an even more general model to encompass all functionalities of chemical and biological interest. Since such future parametrizations and extensions to other elements are anticipated, the present parametrization of PMO is labeled as version 1 or PMOv1 in our computer program. However, since it is the only version currently available, no confusion will occur if we simply call it PMO in the present article.

2. THEORY

As in all popular semiempirical models, only valence electrons are treated explicitly; the nuclei and core electrons (for atoms

Received: November 8, 2010
Published: March 03, 2011

heavier than He) are combined together as the nuclear "core." The core−core interactions are used to describe classical Coulomb energies and to account for the electronic screening effects and the errors in electronic integrals introduced by the NDDO approximation. The core−core repulsion is modeled in an empirical way, even for the core of a hydrogen atom, which is just a nucleus. Valence electrons are treated by a minimum basis set of one s function and a subshell of three p functions on each atom; molecular orbitals are optimized by an iterative self-consistent-field[13] (SCF) calculation.

In principle, semiempirical models are parametrized against experimental data, so that electron correlation effects, including short- and medium-range dynamical correlation effects and long-range dispersion interactions, can be implicitly incorporated into the method by using effective electronic integrals. This has been the strategy employed by Dewar[1] and others in the past; however, significant progress in the understanding of the origin of intermolecular interactions has been made in the past 25 years, especially by using accurate ab initio methods. The relative contribution of dispersion effects to intermolecular interactions can now be accurately estimated for small- to medium-sized systems. A number of recent methods for energy decomposition analysis further helped the understanding of the origin of binding interactions in molecular complexes.[14−17] Thus, we have decided to incorporate empirical dispersion terms as a post-SCF procedure, and in our current implementation, the same functional form is adopted as that used by several groups previously,[10−12,18,19] with the same parameters as used by Grimme[19] and by Hillier and co-workers.[10−12]

Another difference in the present treatment from previous NDDO parametrizations is that we parametrize the electronic energy, including nuclear repulsion, against corresponding benchmark data instead of parametrizing against standard-state enthalpies of formation.

In the NDDO approximation, interatomic differential overlap is neglected in two-electron integrals and in the overlap integrals, but all one-electron integrals are retained, although one-electron as well as two-electron integrals are parametrized rather than evaluated directly.[3]

In MNDO and all other subsequent versions of semiempirical models based on NDDO approximations considered here, two-center electron repulsion integrals are treated as multipole−multipole interactions by the method of Dewar and Thiel.[20] This is also used in PMO except for two-center terms involving p orbitals of hydrogen on both centers. In the MNDO treatment of two-center electron repulsion integrals, the density of a p orbital is represented as the sum of a monopole and a quadrupole charge distribution. In PMO, for integrals involving hydrogen p orbitals on both centers, we retain only the monopole contribution.

Parameters in NDDO methods depend on the atomic numbers of the orbitals involved in the parametrized integral. Because of the NDDO approximation, all three-center and four-center integrals are neglected. For the highest accuracy, all parameters for two-center integrals would be specific to a given pair of atomic numbers (pair parameter scheme, in the language used in ref 4), but in the present paper, as in the original MNDO,[4] we generally use combining rules to obtain two-center parameters from atomic parameters that are independent of the other center (atomic-parameter scheme). For completeness, we summarize below the conventions used for atomic parameters in the MNDO method, after which, we highlight three exceptions where we override the use of atomic parameters by using pair parameters.

There are 12 independent empirical parameters for each atomic number:

- U_{ss}^{A} and U_{pp}^{A}: the one-center, one-electron energies representing the kinetic energy of an s or p electron on center A and its attraction to its own core[3]
- β_{s}^{A} and β_{p}^{A}: atomic parameters responsible for the two-center, one-electron resonance integrals for $l = 0$ (s) and $l = 1$ (p). The resonance integrals are given by[4]

$$\beta_{ll'}^{AA'} = \frac{\beta_{l}^{A} + \beta_{l'}^{A'}}{2}\langle Alm_{l}|A'l'm'_{l'}\rangle \qquad (1)$$

where $|Alm_l\rangle$ denotes an atomic basis function on atom A, l' and $m'_{l'}$ are the angular momentum and magnetic quantum numbers of the electron on the other center A', and $\langle Alm_l|A'l'm'_{l'}\rangle$ is an overlap integral.[4]

- ζ_{s}^{A} and ζ_{p}^{A}: parameters for the exponent in the Slater-type orbitals (STOs) for atom A used to compute the overlap integrals of eq 1 as well as to determine the charge separations in the multipole expansion sites used to evaluate two-center, two-electron integrals.[4] To make the gradients analytic, the STOs are expressed as a linear combination of six Gaussians.[21]
- α^{A}: electronic screening parameters for the exponent in the core−core repulsion terms.[4]
- g_{ss}^{A}, g_{sp}^{A}, g_{pp}^{A}, $g_{pp'}^{A}$, and h_{sp}^{A}: parameters used to establish the one-center limits of the Coulomb (g) and exchange (h) integrals as $R_{AA'} \rightarrow 0$ of the Dewar−Sabelli−Klopman approximation to the two-center, two-electron integrals, where $R_{AA'}$ is the internuclear distance between atoms A and A'.[22] Another exchange integral is also needed, but in order to maintain rotational invariance, it is given by

$$h_{pp'}^{A} = \frac{g_{pp}^{A} + g_{pp'}^{A'}}{2} \qquad (2)$$

As mentioned above, in three cases, exceptions were made to using the standard MNDO functional forms on the basis of atomic parameters:

(1) For the resonance integrals involving p orbitals on hydrogen atoms, we override eq 1 with

$$\beta_{pp}^{HH'} = 0 \qquad (3a)$$

$$\beta_{sp}^{HH'} = 0 \qquad (3b)$$

$$\beta_{lp}^{OH} = P_1\frac{\beta_{l}^{O} + \beta_{p}^{H}}{2}\langle Olm_{l}|H1m'_{l'}\rangle \qquad (4)$$

where l'=1 and P_1 is a parameter. Furthermore, for the H−H resonance integrals, we use a specific value ζ_{l}^{HH} of ζ_{l}^{H}, and for the O−O resonance integrals, we use a specific value ζ_{l}^{OO} of ζ_{l}^{O}.

(2) For the two-center, one-electron attraction integrals between an electron in a distribution on atom H and the core of another hydrogen atom B (where $B \neq$ H but $Z_B = 1$), for which we use the ab initio notation $\langle Hlm_l|-Z_B/r_B|Hlm'_{l'}\rangle$, in which l is 1 and r_B is the distance of the electron on H from B, the standard MNDO result is

Table 1. Parameters

parameter	PMO	MNDO	AM1	PM3	PDDG/PM3	RM1	PM3-D	PM6
U_{ss}^{H} (eV)	−11.22813	−11.91	−11.40	−13.07	−12.89	−11.96	−13.05	−11.25
U_{pp}^{H} (eV)	−9.95254							
β_S(eV))	−6.89857	−6.99	−6.17	−5.63	−6.15	−5.77	−5.63	−8.35
β_p^H (eV)	−3.77765							
ζ_s^H (bohr^{-1})	1.08419	1.33	1.19	0.97	0.97	1.08	0.97	1.27
ζ_p^H (bohr^{-1})	0.88997							
α^H (Å^{-1})	3.16046	2.54	2.88	3.36	3.38	3.07	3.42	...
g_{ss}^H (eV)	12.65697	12.85	12.85	14.79	14.79	13.98	14.79	14.45
g_{sp}^H (eV)	11.34825							
g_{pp}^H (eV)	6.17416							
$g_{pp'}^H$ (eV))	10.0441							
h_{sp}^H (eV)	2.32560							
U_{ss}^{O} (eV)	−114.78169	−99.64	−97.83	−86.99	−87.41	−96.95	−86.96	−91.68
U_{pp}^{O} (eV)	−78.04828	−78.30	−78.26	−71.88	−72.18	−77.89	−71.93	−70.46
β_s^O (eV)	−31.51770	−32.69	−29.27	−45.20	−44.87	−29.85	−45.23	−65.64
β_p^O (eV)	−35.10436	−32.69	−29.27	−24.75	−24.60	−29.15	−24.79	−21.62
ζ_s^O (bohr^{-1})	3.19623	2.70	3.11	3.80	3.81	3.18	3.80	5.42
ζ_p^O (bohr^{-1})	3.11976	2.70	2.52	2.39	2.32	2.55	2.39	2.27
α^O (Å^{-1})	3.44202	3.16	4.46	3.22	3.23	4.17	3.39	...
g_{ss}^O (eV)	18.22143	15.42	15.42	15.76	15.76	14.00	15.76	11.30
g_{sp}^O (eV)	12.73220	14.52	14.52	10.62	10.62	14.96	10.62	15.81
g_{pp}^O (eV)	15.03924	14.48	14.48	13.65	13.65	14.15	13.65	13.62
$g_{pp'}^O$ (eV)	13.52768	12.98	12.98	12.41	12.41	12.70	12.41	10.33
h_{sp}^O (eV)	4.19786	3.94	3.94	0.59	0.59	3.93	0.59	5.01

specifically screened when the two atoms are in close proximity:

$$\left\langle \mathrm{H}lm_l \left| -\frac{Z_B}{r_B} \right| \mathrm{H}lm'_{l'} \right\rangle_{\mathrm{PMO}} = \left\langle \mathrm{H}lm_l \left| -\frac{Z_B}{r_B} \right| \mathrm{H}lm'_{l'} \right\rangle_{\mathrm{MNDO}} [1 + P_2 \exp(-P_3 R_{\mathrm{HH}'}^2)] \quad (5)$$

where P_2 is negative. Note that the standard MNDO approximation,[4] $\langle \mathrm{H}lm_l|-Z_B/r_B|\mathrm{H}lm'_{l'}\rangle_{\mathrm{MNDO}}$, of this one-electron attraction integral is calculated from the two-electron integral $\langle Bs0Bs0|\mathrm{H}lm_l\mathrm{H}lm'_{l'}\rangle$ (where we use the Mulliken convention for two-electron integrals), but the screening of eq 5 is applied to the one-electron integral (when B is a hydrogen and l is 1) and not to the two-electron integral.

(3) For the homonuclear core−core repulsion integrals, we replace α^O and α^H by $\hat{\alpha}^O$ and $\hat{\alpha}^H$, respectively, whereas the heteronuclear core−core repulsions are computed from the atomic parameters α^O and α^H.

The parameters in the damped dispersion terms were retained from earlier work[10−12,15] without change (in particular, they are the same as in MNDO-D and PM3-D from the Hillier group). MNDO parameters and the new PMO parameters (U_{pp}^H, β_p^H, ζ_p^H, g_{sp}^H, g_{pp}^H, $g_{pp'}^H$, h_{sp}^H, P_1, P_2, P_3, $\hat{\alpha}^O$, and $\hat{\alpha}^H$) were adjusted by iterative optimizations using a genetic algorithm, in the presence of the dispersion term and the p orbitals on hydrogen atoms, to give a subjectively reasonable compromise in the accuracy of a lot of benchmark data. The final PMO values of the MNDO parameters, including those for p orbitals on H, are given in Tables 1 and 2. The parameters in Table 1 are those that may be compared to the parameters of other NDDO methods, and they are compared to MNDO,[4] AM1,[1] PM3,[2] PDDG-PM3,[23] RM1,[24] PM3-D,[10] and PM6.[25] Note that in Table 1, the parameters of PMO are given to the number of digits that define the parametrization, but for the other methods, the numbers are truncated to two places after the decimal point (calculations with the other methods employed the full number of digits, but the values for other methods in Table 1 are just for comparison, and they are rounded so that the essential features and trends are more apparent). The parameters in Table 2 are additional PMO parameters that do not appear in older methods.

Table 2. Additional PMO Parameters

parameter	value
P_1	0.15
P_2	−0.75
P_3	1.1 Å^{-2}
$\hat{\alpha}^O$	3.304 Å^{-1}
$\hat{\alpha}^H$	2.466 Å^{-1}
ζ_l^{HH}	1.280 bohr^{-1}
ζ_l^{OO}	2.764 bohr^{-1}

The choice of functional forms in eqs 3a−5 was based on our experiences with parametrization. In particular, we tried several other functional forms and several other strategies for which terms to modify, and we selected the ones above because they are physically reasonable and they work well.

dx.doi.org/10.1021/ct100638g |J. Chem. Theory Comput. 2011, 7, 857–867

Table 3. Results

species	quantity	reference	source[a]	PMO	MNDO	AM1	PM3	PDDG/PM3	RM1	PM3-D	PM6
H_2O	AE (kcal/mol)	232.2	27;28	233.0	225.0	223.0	217.2	245.4	221.6	246.5	218.0
	IP (eV)	12.68	29;28,30	12.00	11.76	11.95	12.05	12.31	11.82	12.11	11.45
	r (Å)	0.96	31	0.96	0.94	0.96	0.95	0.95	0.96	0.93	0.95
	θ (deg)	104.5	31	104.6	106.8	103.5	107.7	105.4	103.4	108.9	107.5
	α (Å^3)	1.45	32	1.24	0.43	0.50	0.50	0.49	0.51	0.46	0.40
	q^O	...[b]	...	−0.40	−0.33	−0.38	−0.36	−0.39	−0.37	−0.37	−0.62
	q^H	...	...	0.20	0.16	0.19	0.18	0.19	0.18	0.19	0.31
	μ (Debye)										
	Mulliken	...	32	1.13	0.88	1.09	0.97	1.08	1.05	0.96	1.67
	hybrid	...	...	1.06	0.90	0.77	0.77	0.75	0.82	0.78	0.40
	total	1.85	33	2.19	1.78	1.86	1.74	1.84	1.87	1.74	2.07
$(H_2O)_2$	BE (kcal/mol)[c]	5.0	34	4.7	1.0	5.5	3.5	3.7	2.8	6.5	4.9
	r_{14} (Å)	0.97	35	0.97	0.94	n.q.c.[d]	0.96	0.97	n.q.c.	0.94	n.q.c.
	r_{13} (Å)	0.96	35	0.96	0.94	n.q.c.	0.95	0.95	n.q.c.	0.93	n.q.c.
	r_{24} (Å)	1.95	35	1.96	3.42	n.q.c.	1.81	1.71	n.q.c.	1.77	n.q.c.
	r_{25} (Å)	0.96	35	0.97	0.94	n.q.c.	0.95	0.96	n.q.c.	0.93	n.q.c.
	θ_{413} (deg)	104.5	35	103.9	106.8	n.q.c.	107.7	105.3	n.q.c.	108.8	n.q.c.
	θ_{142} (deg)	172.9	35	173.4	114.0	n.q.c.	179.6	178.2	n.q.c.	172.1	n.q.c.
	θ_{126}(deg)	110.4	35	112.0	130.4	n.q.c.	110.6	113.2	n.q.c.	113.3	n.q.c.
$(H_2O)_2$	μ (Debye)										
	Mulliken	...		1.76	1.80	2.34	1.63	1.96	2.20	1.78	1.49
	hybrid	...		1.42	1.81	1.52	0.86	0.87	1.63	0.98	0.38
	total	2.65	36	3.11	3.60	3.86	2.49	2.83	3.83	2.76	1.87
H_2	AE (kcal/mol)	109.5	37	108.2	103.8	109.7	117.6	137.0	106.1	119.9	129.8
	IP (eV)	15.55	38;39	13.60	14.72	14.19	15.53	15.85	14.33	15.56	14.17
	r (Å)	0.74	37	0.70	0.66	0.68	0.70	0.68	0.70	0.69	0.76
OH^-	AE (kcal/mol)	115.4	40,41;39	116.7	117.4	125.8	129.2	149.8	121.2	144.9	144.7
	IP (eV)	1.83	42;39	2.18	0.27	0.65	0.89	1.16	0.55	0.92	2.05
	r (Å)	0.96	43	0.88	0.94	0.94	0.94	0.94	0.94	0.92	0.87
H_3O^+	r (Å)	0.98	44	1.02	0.96	1.00	0.98	0.98	0.99	0.95	1.04
	θ (deg)	111.3	44	104.1	115.3	107.8	109.4	106.5	109.5	110.8	102.0

[a] When more than one source is cited, the source(s) before the semicolon is (are) for the value at 0 K, and the source(s) after the semicolon is (are) for the zero point energy used to convert it to a potential energy difference. [b] ... denotes not applicable. [c] BE = binding energy = 2(energy of the gas-phase water monomer optimized with the given method) − (energy of the gas-phase water dimer optimized with the given method). [d] The geometrical parameters of the water dimer are not given for AM1, RM1, and PM6 because the structure is not qualitatively correct (n.q.c.).

It is worthwhile to also mention another choice issue here, namely, the choice of p basis functions on hydrogen atoms rather than (for example) d basis functions on nonhydrogenic atoms, which may have seemed a more obvious choice. The introduction of d basis functions on nonhydrogenic atoms has been considered previously,[26] and these functions are known to improve the description of small rings and of some structures containing elements from the 3p block. Here our goal is an improved description of polarizability, even for compounds with atoms no heavier than the 2p block, and the choice of p basis functions on hydrogen is motivated by the results of part 1. Note that our goal is to achieve the best performance at a minimal increase in computational cost; this balance favors a set of p orbitals on hydrogenic atoms.

3. RESULTS

The computed results for molecules and for various water dimer configurations are listed in Tables 3−6, along with the reference data (i.e., the most accurate available data) for comparison. The following abbreviations are used throughout: AE, atomization energy; IP, ionization potential; r, bond distance; θ, bond angle; α, polarizability; μ, dipole moment; and BE, bond energy. The reference data in Table 3 are based on previous work, usually experimental, but we needed to convert experimental energetic quantities (AE and BE) from enthalpy differences at 0 K to potential energy differences by subtracting zero point energies, based on experimental spectra or theoretical estimates. The third column of the table gives details of the sources[27−44] of all reference data.

Table 3 shows that the polarizability of water is now much more accurate than that from previous NDDO methods. In fact, we can find parameters that make it perfect, while still yielding reasonable results for other data, but our final parameters are a compromise in which we accept a 14% error in water's polarizability in order to retain good accuracy for other quantities.

Table 3 also shows remarkably good accuracy for the atomization energy (AE) of water, the bond energies of key diatomics, and the ionization potential (IP) and the geometry of water and key diatomics. Fitting simultaneously the dipole moment and

Table 4. Potential Curves[a] for Water Dimer in Hydrogen Binding Orientation (kcal/mol)

d(H−O) (Å)	PMO	AM1	MNDO	PM3	RM1	PM6	PM3-D	PDDG-PM3	M06-2X/MG3S	CCSD(T)-F12b/aug-cc-pVTZ
0.948	83.1	88.9	122.1	61.9	72.3	74.9	39.6	61.2	82.0	83.6
1.248	16.6	26.2	47.1	22.2	13.6	15.2	11.3	17.7	15.5	16.8
1.448	2.6	11.8	27.2	9.3	2.9	1.6	2.5	4.7	1.7	2.4
1.648	−2.7	3.0	15.9	−1.3	−0.5	−2.9	−5.6	−3.3	−3.7	−3.5
1.948	−4.6	−2.8	6.7	−2.8	−0.9	−3.9	−5.1	−1.1	−5.5	−5.1
2.448	−3.7	−2.5	0.8	−1.7	−1.8	−2.8	−2.5	−1.9	−4.0	−3.8
2.948	−2.5	−1.3	−0.5	−1.1	−1.2	−1.7	−1.5	−1.3	−2.5	−2.3
3.948	−1.1	−0.6	−0.5	−0.5	−0.6	−0.8	−0.6	−0.6	−1.0	−0.9
4.948	−0.6	−0.3	−0.3	−0.3	−0.3	−0.5	−0.3	−0.3	−0.5	−0.5
5.948	−0.3	−0.2	−0.2	−0.2	−0.2	−0.3	−0.2	−0.2	−0.3	−0.3
6.948	−0.2	−0.1	−0.1	−0.1	−0.1	−0.2	−0.1	−0.1	−0.2	−0.2

[a] The energies shown are relative to the energy of the dimer when d(H−O) = 99 Å.

Table 5. Potential Curves[a] for Water Dimer in Repulsive Overlay Orientation (kcal/mol)

d(O−O) (Å)	PMO	AM1	MNDO	PM3	RM1	PM6	PM3-D	PDDG-PM3	M06-2X/MG3S	CCSD(T)-F12b/aug-cc-pVTZ
2.0	40.5	12.9	44.4	13.7	23.2	16.3	5.9	20.4	43.5	44.5
2.5	10.0	1.2	11.3	4.0	2.7	3.9	1.2	2.9	9.1	10.1
3.0	3.5	1.5	3.6	1.7	1.6	2.5	0.6	1.6	2.9	3.1
4.0	1.3	0.8	0.8	0.7	0.8	0.9	0.5	0.7	0.9	0.9
5.0	0.7	0.4	0.4	0.4	0.4	0.5	0.3	0.4	0.5	0.5
6.0	0.4	0.2	0.2	0.2	0.2	0.3	0.2	0.2	0.3	0.3

[a] The energies shown are relative to the energy of the dimer when d(O−O) = 99 Å.

Table 6. Interaction Energies (kcal/mol) at Water Dimer Stationary Points[a]

structure	PMO	AM1	MNDO	PM3	RM1	PM6	PM3-D	PDDG-PM3	reference[b]
nonplanar open C_s	−4.7	−2.8	7.5	−2.4	−0.9	−3.7	−2.3	−1.0	−5.0
open C_1	−4.1	−2.2	7.3	−1.4	−0.2	−2.9	−1.2	0.3	−4.5
planar open C_s	−4.1	−2.4	6.7	−1.4	−0.5	−3.0	−1.1	0.4	−4.4
cyclic C_i	−2.7	−3.8	7.6	−0.2	−0.2	−3.4	0.2	0.8	−4.3
cyclic C_2	−2.3	−3.4	7.8	0.3	0.2	−2.9	0.7	1.2	−4.0
cyclic C_{2h}	−2.3	−3.5	7.6	0.4	0.0	−3.1	0.7	1.3	−4.0
triply H bonded C_s	−2.7	−3.8	3.7	−1.2	−2.6	−2.8	−0.6	−1.1	−3.2
doubly bifurcated C_{2h}	−1.3	−1.6	1.9	−0.6	−1.3	−1.0	0.5	−1.5	−1.4
nonplanar bifurcated C_{2v}	−3.0	−3.7	2.8	−1.2	−2.8	−3.0	−0.3	−2.3	−3.2
planar bifurcated C_{2v}	−2.6	−2.9	1.6	−1.1	−2.5	−2.3	0.0	−2.4	−2.3
mean unsigned deviation	0.7	1.0	9.1	2.7	2.6	0.8	3.3	3.2	

[a] All interaction energies in this table are with respect to two separated monomers at the monomer geometry of ref 35. [b] Coupled cluster value from ref 35.

molecular polarizability of water is problematic and requires a compromise in consideration of various aspects of applications in the gas phase and in condensed phases. On one hand, the total dipole moment is calculated from the wave function, which is a sum of two contributions in the NDDO approximation: one from the partial charges formally equivalent to those by Mulliken analysis and one from the hybridization terms in the dipole matrix elements. On the other hand, the wave functions of semiempirical models that employ a minimal basis set tend to severely underestimate the charge separations of polar bonds, resulting in Mulliken population charges or electrostatic-potential-fitted charges that are too small for use in condensed-phase simulations. From the latter perspective, it is not critical to enforce a perfect agreement with the experimental dipole moment of an isolated water molecule in the gas phase; in fact, it is desirable to have a somewhat enhanced molecular dipole moment in view of the limitations of a minimal basis set for describing polar bonds. The compromise we chose is to simply require that the experimental dipole moment lies between the Mulliken and total values.

The final data to be discussed in Table 3 are those for the water dimer. Several previous NDDO methods give qualitatively incorrect geometries for the water dimer. The water dimer structures for all of the NDDO methods are shown in Figure 1, and these structures may be compared to the best estimate[35] of the water dimer structure, which is shown in Figure 2. PMO not only gives the qualitatively correct structure but gives reasonably accurate geometrical parameters, as shown in Table 3. Furthermore, the reference value for the dipole moment of the water dimer is between the Mulliken and total values calculated by PMO.

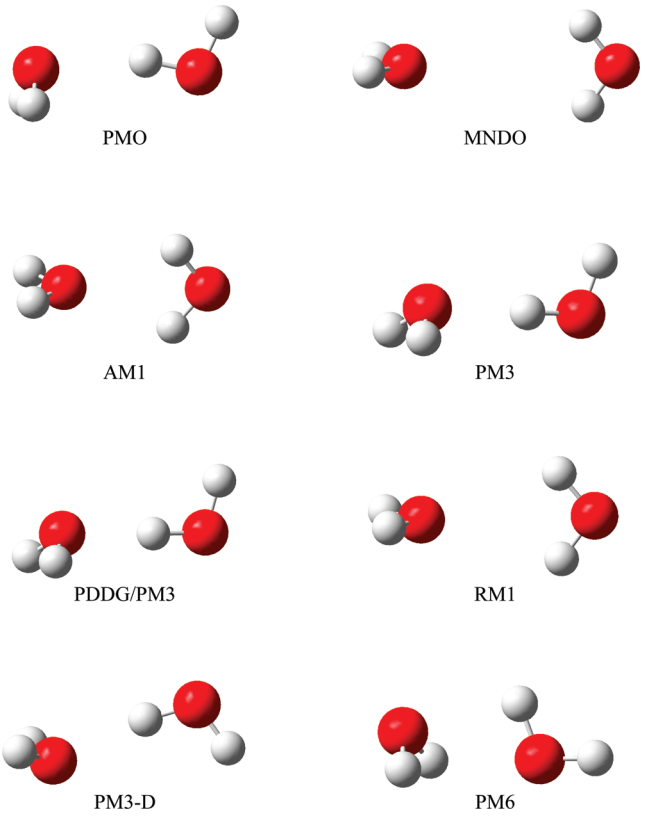

Figure 1. Equilibrium water dimer structure predicted by various semiempirical electronic structure methods.

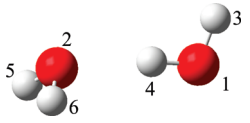

Figure 2. Best estimate of the structure of the minimum-energy water dimer from ref 35.

A key issue in parametrizing semiempirical methods is to achieve a realistic combination of noncovalent attractive interactions and exchange repulsion. This has led to a variety of special terms being added to the core−core repulsion, including Gaussian modification terms.[1,2,23] The performance of PMO to predict the interaction energy between two water molecules over a wide range of separation distances is discussed next.

We consider two relative orientations of the water molecules, one being the hydrogen bonded orientation and the other, shown in Figure 3, being a structure that we will label the repulsive overlay. For the hydrogen bonded orientation, we start with the optimum dimer structure of Tschumper et al., and we pull the monomers apart along the O−H hydrogen bond direction. For the repulsive overlay, we make the planes of the two monomers parallel, with one water molecule precisely aligned with the other one. In the first case, the interaction energy is determined as a function of the O−H hydrogen bond distance, d(O−H), and in the second, it is calculated as a function of the O−O distance, d(O−O). In both cases, we calculated the potential energy curve, relative to the separated monomers, by two high-level methods. Note that the monomers are rigid in both structures. For the hydrogen bonded structures, they are rigid at the geometries they

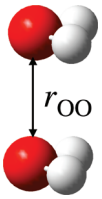

Figure 3. "Repulsive overlay" water dimer.

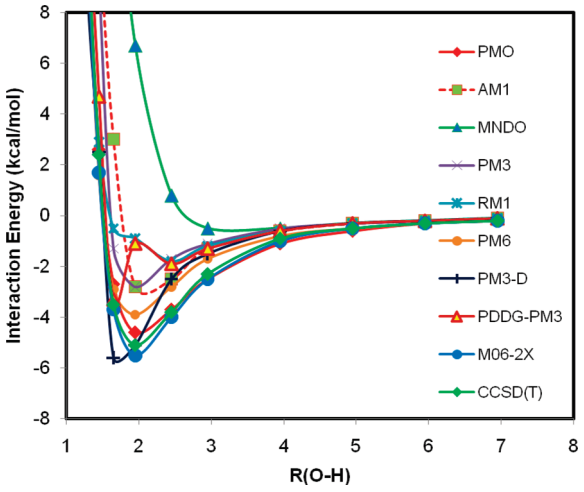

Figure 4. Potential energy curves (kcal/mol) for the hydrogen-bonding configuration of a water dimer computed using various semiempirical, ab initio wave function, and density functional methods, as labeled in the figure. Distances are shown in angstroms.

have in the dimer structure of Tschumper et al., and for the repulsive overlay they are rigid at the experimental geometry[45] of the gas-phase water monomer. We use the same geometries for the NDDO calculations and the high-level calculations. The high-level calculations are carried out by the M06-2X density functional[46] with the MG3S[47] basis and by the high-level CCSD(T)-F12b[48] ab initio wave function method with the aug-cc-pVTZ[49] basis set. The latter should be close to the complete configuration interaction limit.

Table 4 and Figure 4 show that only PMO and PM6 give reasonably accurate potential curves for the hydrogen bonding orientation, although the binding energy from PM6 is 1 kcal/mol too weak in comparison with CCSD(T) results. The other methods are not attractive enough, as seen by their prediction of highly repulsive interactions at hydrogen-bonding distances, a shortfall of the original MNDO method that led to the introduction of Gaussian terms in the core−core potential in the highly successful AM1 model. PM3-D was developed by adjusting some of the original PM3 parameters after damped dispersion terms are introduced, which yields an excellent binding energy, but the hydrogen-bond distance at the minimum-energy geometry is too short, and the potential energy curve dies off too quickly at medium distances. The recently introduced RM1 model produced a minimum that is too far away for a good single hydrogen-bonded complex and a shoulder with a much higher energy at a distance shorter than the best estimate of the minimum. This is reflected in the minimum energy configuration obtained with RM1 (Figure 1), showing a bifurcated complex—a deficiency that is also well-known for a water dimer in the MNDO and AM1 models. Table 5 shows that only PMO and MNDO give

reasonable potential energy curves in the repulsive overlay orientation, with the other curves not being repulsive enough. Thus, the present parametrization succeeds in representing these opposing types of interactions well, over a wide range of distances.

Next, we consider a broad set of water dimer geometries. In particular, Table 6 gives results at the geometries of all 10 stationary points on the water dimer surface that were characterized by Tschumper et al.[35] at the coupled cluster level, where only one structure is a minimum and the others consist of three first-order saddle points and six higher-order saddle points (hilltops); the names of the structures are those given to them in ref 35, and the structures are illustrated in Figure 5. Our comparisons are carried out at these geometries without any reoptimization; the goal is not to test what set of stationary structures is predicted by the methods but rather to test whether the potential energy surface is well reproduced over a range of geometries at various locations on the high-dimensional potential energy surface. The table shows that PMO gives a qualitatively correct description of the various interaction energies, and it is in better agreement with the accurate results than any previous NDDO method, although AM1 ad PM6 do almost as well.

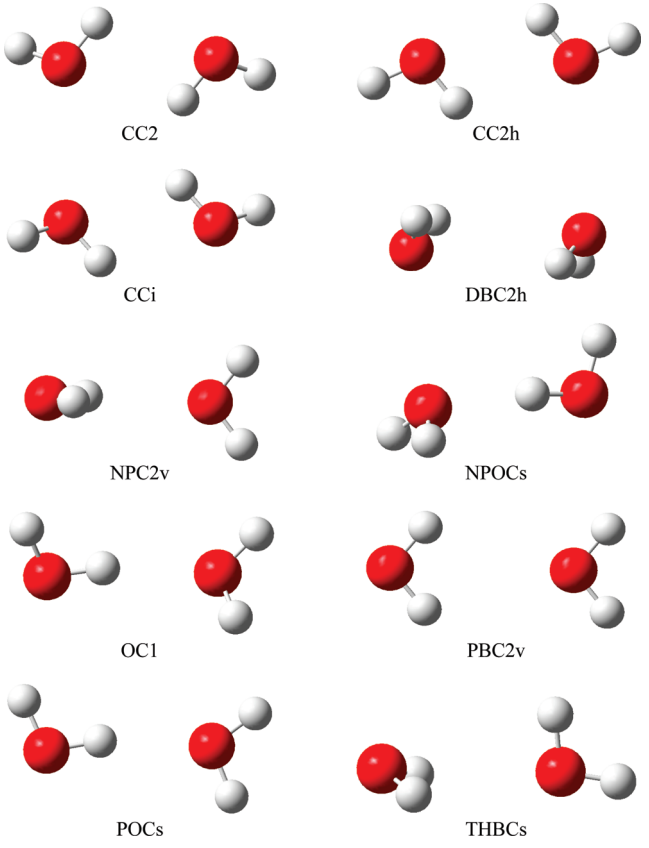

Figure 5. Stationary points on the water dimer potential energy surface from ref 35.

Tables 7 and 8 present results for larger water clusters, up to the octamer. These larger clusters are a severe test of the ability of the PMO model to include nonadditive polarization effects such as those that occur when a monomer interacts with other monomers in more than one direction. Table 7 shows the energies computed with each semiempirical model using the structures from the work of Bryantsev et al.,[50] who used density functional theory (DFT) geometries and relative energies obtained by high-level (CCSD(T)) ab initio wave function theory.

Whereas Table 7 is a comparison of interaction energies using the set of fixed structures from ref 50, Table 8 provides a different kind of test. For Table 8, the results were obtained with the fully optimized structures for these clusters at each semiempirical level; the structures of ref 50 were used as the starting points, and the nearest lower-energy stationary points were sought for each semiempirical model using the default geometry optimizer in the MOPAC[51] software program, which is based on a modified Broyden−Fletcher−Goldfarb−Shanno (BFGS) method.[52] (A configuration was considered optimized when its gradient norm fell below 0.5 kcal mol^{-1} Å^{-1}.) The PMO optimized structures obtained by this procedure are shown in Figure 6, whereas those from other models are supplied in the Supporting Information. Only the PMO calculations yield cluster structures that closely resemble those of the DFT results of Bryantsev et al.[50] Furthermore, for PMO, the agreement is very good for all cluster configurations. The data in Table 7 are quite revealing of the deficiencies exhibited in each semiempirical model. As expected on the basis of results for the dimer complex (Table 4), MNDO gives strongly repulsive interactions for these clusters at hydrogen-bonding geometries. In fact, at these fixed hydrogen-bonding configurations, none of the previous

Table 7. Interaction Energies (kcal/mol) of Water Clusters from Single-Point Calculations Using the Fixed Geometries from Ref 50[a]

structure	PMO	AM1	MNDO	PM3	RM1	PM6	PM3-D	PDDG-PM3	reference
$(H_2O)_2$	−4.6	−2.9	7.1	−2.5	−0.9	−3.8	−4.3	−0.9	−5.0
$(H_2O)_3$ cycle	−8.3	−2.3	40.6	−9.2	−1.4	−11.8	−20.9	−7.5	−15.8
$(H_2O)_4$ cycle	−25.1	−5.8	45.0	−17.8	−6.7	−20.7	−28.5	−17.1	−27.4
$(H_2O)_5$ cycle	−28.1	2.2	70.2	−18.6	−9.4	−24.5	−40.0	−25.1	−35.9
$(H_2O)_6$ cycle	−41.3	−4.9	68.6	−27.5	−14.4	−32.8	−44.6	−30.6	−44.3
$(H_2O)_6$ cage	−42.2	−16.0	78.0	−24.5	−7.0	−33.9	−44.2	−17.8	−46.0
$(H_2O)_6$ book	−42.2	−10.1	74.8	−26.8	−10.3	−33.5	−45.2	−24.6	−45.8
$(H_2O)_6$ prism	−42.3	−21.1	76.5	−21.9	−7.4	−34.9	−41.8	−14.4	−45.3
$(H_2O)_8 D_{2h}$	−69.1	−22.6	121.4	−39.5	−12.4	−53.9	−70.6	−30.3	−72.6
mean unsigned deviation	3.9	28.3	102.3	16.6	29.8	9.8	2.1	18.9	

[a] Structures and reference energies from ref 50. The interaction energy is calculated relative to the infinitely separated gas-phase monomers with geometries frozen in the monomer geometry given in ref 50.

dx.doi.org/10.1021/ct100638g |J. Chem. Theory Comput. 2011, 7, 857–867

Table 8. Interaction Energies (kcal/mol) of Water Clusters Computed Using the Optimized Structures at Each Theoretical Model[a]

Structure	PMO	AM1	MNDO	PM3	RM1	PM6	PM3-D	PDDG-PM3	reference
$(H_2O)_2$	−4.7	−5.5	−1.0	−3.5	−2.8	−4.9	−6.5	−3.7	−5.0
$(H_2O)_3$ cycle	−13.4	−15.3	−1.6	−10.1	−4.0	−13.3	−19.8	−10.2	−15.8
$(H_2O)_4$ cycle	−26.0	−22.1	−3.1	−18.3	−10.0	−22.3	−31.8	−21.1	−27.4
$(H_2O)_5$ cycle	−34.7	−31.8	−4.7	−23.8	−14.5	−29.4	−40.8	−28.0	−35.9
$(H_2O)_6$ cycle	−42.6	−32.8	−5.1	−29.2	−18.3	−36.0	−49.1	−34.5	−44.3
$(H_2O)_6$ cage	−43.9	−30.2	−4.8	−30.2	−16.1	−37.5	−60.9	−34.7	−46.0
$(H_2O)_6$ book	−43.6	−38.9	−5.0	−30.0	−17.7	−35.1	−54.6	−34.9	−45.8
$(H_2O)_6$ prism	−43.9	−39.4	−4.3	−29.7	−16.4	−39.3	−62.5	−35.0	−45.3
$(H_2O)_8D_{2\ h}$	−72.4	−56.5	−6.9	−48.6	−24.0	−58.1	−93.8	−56.6	−72.6
Mean unsigned deviation	1.5	7.4	33.5	12.8	23.8	6.9	9.1	8.8	

[a] The starting geometries in all structural optimizations are taken from the DFT optimized geometries in ref 50. Reference energies are taken from ref 50. The interaction energy is calculated relative to the infinitely separated gas-phase monomers with geometries optimized with the given method.

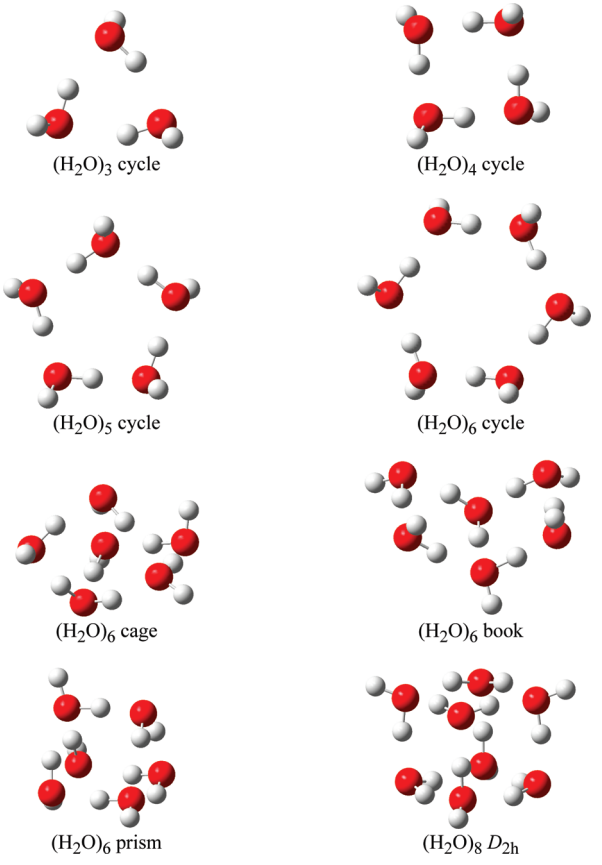

Figure 6. Optimized water clusters using the PMO method.

semiempirical models are attractive enough in comparison with CCSD(T) results, except PMO and PM3-D, in which dispersion energies are explicitly modeled. The interaction energies for the optimized structures do not show noticeable improvement after the structures are fully relaxed in each previous semiempirical model; as it turns out, AM1 and PM6 perform the best for the larger clusters, whereas the binding energies from PM3-D become too large for the larger water clusters. Table 8 shows that the mean unsigned error of the present PMO method is only 1.5 kcal/mol for these water clusters. The success of the PMO model for the cluster energetics at consistently optimized geometries is a crowning achievement for the method.

Table 9. Dispersion Contributions to the Energies of Water Clusters[a]

	at geometries of Table 7				at geometries of Table 8			
structure	PMOxD	D	PMO	%D	PMOxD	D	PMO	%D
$(H_2O)_2$	−3.8	−0.8	−4.6	17	−3.9	−0.8	−4.7	17
$(H_2O)_3$ cycle	−5.9	−2.4	−8.3	29	−11.0	−2.4	−13.4	18
$(H_2O)_4$ cycle	−21.3	−3.8	−25.1	15	−21.9	−4.1	−26.0	16
$(H_2O)_5$ cycle	−23.2	−4.9	−28.1	17	−29.6	−5.1	−34.7	15
$(H_2O)_6$ cycle	−35.6	−5.7	−41.3	13	−36.6	−6.0	−42.6	14
$(H_2O)_6$ cage	−33.6	−8.6	−42.2	20	−35.0	−8.9	−43.9	20
$(H_2O)_6$ book	−35.0	−7.2	−42.2	17	−36.3	−7.3	−43.6	17
$(H_2O)_6$ prism	−33.2	−9.1	−42.3	22	−34.8	−9.1	−43.9	21
$(H_2O)_8D_{2h}$	−55.7	−13.4	−69.1	19	−57.9	−14.5	−72.4	20
mean percentage	...	...	...	19	...	...	...	18

[a] Energies are in kcal/mol, and %D is defined as (D/PMO) × 100%.

A question of interest in parametrization is how much the damped dispersion term contributes to the results. This is illustrated for the water clusters in Table 9. In this table, PMOxD is the result obtained excluding the damped dispersion term. D denotes the contribution of the damped dispersion term, and PMO is the total. Results are shown both for the accurate geometries of Table 7 and for the consistently optimized geometries of Table 8. We see that the dispersion contribution ranges from 13 to 22% of the total binding energy, with the percentage not depending strongly on cluster size. The average, shown in the last row, is almost 20%. We may compare the present result for the damped dispersion energy at the equilibrium geometry of the dimer to the percentage estimated by the ab initio second-order symmetry-adapted perturbation theory (SAPT2), which yields a damped dispersion contribution of −2.49 kcal/mol, or 46% of the total interaction energy of the cluster (−5.4 kcal/mol) computed at that level of approximation.[53] Note that the damped dispersion component is not uniquely defined; the quantity called dispersion in SAPT2 includes all correlation effects on the direct induction energy[53] (and hence it may also be called the correlation contribution to the direct induction/dispersion). Su and Li[54] use different definitions; they label the sum of all four correlation components of SAPT2 (direct static, direct induction/dispersion, exchange static, and exchange remainder) as dispersion; applying the

Table 10. Proton Transfer Energies (kcal/mol) for $A + H_3O^+ \rightarrow AH^+ + H_2O$[a]

A	PMO	MNDO	AM1	PM3	PDDG/PM3	RM1	PM3-D	PM6	reference	source
H_2	27.7	63.8	26.4	16.1	4.9	27.8	25.4	−7.3	66.7	51
OH^-	−220.0	−250.3	−247.8	−248.4	−248.3	−246.6	−249.8	−216.7	−223.1	27, 41, 42, 52
OH	17.1	14.6	12.6	8.9	8.7	13.2	8.3	0.1	26.0	41
H_2O_2	7.6	20.5	11.7	3.2	9.6	15.8	8.5	0.5	9.7	41, 42, 53
HO_2	13.8	17.6	10.2	0.5	2.0	10.8	3.6	−7.1	7.8	51
O_3	20.3	109.5	108.5	100.5	111.0	106.1	97.4	−8.9	17.4	51
MUD[b]	10.3	25.7	29.0	31.7	34.0	28.8	28.5	26.1		

[a] For all NDDO calculations in this table, the geometry of each reactant and product was optimized at the level under consideration. [b] Mean unsigned deviation from reference values, which are based on the sources indicated in the last column.

Su−Li definition[54] to the Rybak et al.[53] calculation would yield a "dispersion" contribution of −1.9 kcal/mol or 35%. Given the nonuniqueness of the damped dispersion contribution, the present results in Table 8 are physically reasonable.

The relative proton affinities (excluding, as in all other comparisons in this article, the zero point and thermal vibrational energy) are examined by considering the energy change of proton transfer reactions from an oxonium ion to different bases. Since these reactions involve charge migrations, they present another challenge for methods to adequately treat polarization effects. Table 10 compares the results of NDDO calculations to the reference data, which are obtained by combining data for A and AH+ (in the notation of the table heading) from a number of sources[27,41,42,55−57] with the proton affinity of water[58] and removing vibrational contributions. The table shows that PMO yields better agreement with the reference results than do previous NDDO models.

4. DISCUSSION

As mentioned in section 2, the parametrization reported here represents a compromise. For example, we could find parameters that give the precisely correct polarizability and dipole moment of water; however, it would yield somewhat less accurate interaction energy curves for water dimers and binding energies of water cluster than those in Tables 3−5. We also compromised on fitting the dipole moment of water, simply requiring the accurate value (1.85 D) to lie between the value (1.13 D) calculated from the Mulliken charges and the value (2.19 D) calculated when including the so-called hybrid terms (that is, the atomic dipole terms). Another compromise is that we could obtain more accurate results for water dimers and clusters, but at the expense of lowering the polarizability of water and allowing the dipole moment of water to deviate somewhat from the experimental value. Our final compromise is to require that the polarizability of water is accurate to within 15%.

The inclusion of polarization in force fields used for molecular simulation makes them more realistic, but including polarization in a molecular mechanics framework often involves approximations of uncertain physicality such as the introduction of artificial charge centers, dual thermostatting in shell-type models, and the need to partition the polarizability into atomistic contributions.[59−64] The quantum mechanical framework presented here avoids such devices and represents the polarizability naturally in an SCF framework. Polarization is an important consideration in parametrizing model chemistries. In a liquid, the dielectric screening of electrostatics on average increases the magnitudes of partial atomic charges and dipole moments of neutral molecules. Thus, for a nonpolarizable model, the effective charges are typically parametrized to yield molecular dipole moments about 15% to 20% greater than those in the gas phase; ideally this value would be determined by carrying out simulations on liquids. With polarizable force fields, there is a much greater chance of incorporating polarization effects in response to the instantaneous fluctuations of surrounding solvent and in response to changes in the local electrical field, and thus there is a greater chance that a model can be reasonable both for molecules and small clusters, on the one hand, and for liquids, on the other. In fact, the success of the present model for water clusters ranging from dimers to octamers is already encouraging. Future tests on liquid water would be very interesting.

The parameters presented here are illustrative of the performance with the present theoretical model in its simplest form. It is anticipated that further refinement in parametrization and improved functional form will be found in future work. For example, the two-center terms can be optimized specifically for each pair as a function of the internuclear distance rather than using atomic parameters, or different functional forms may be adopted for different pairs; for example, one can use the pairwise core−core repulsion form suggested by Voityuk and Rösch.[65] Clearly, the next step is to extend the current model to a much larger data set and to a broader range of functional groups. The dispersion terms used in the present PMO model were taken directly from previous work; other functional forms[66−68] and parameters may be fully optimized for complex systems. For condensed-phase simulations, such as liquid water, it is critical to evaluate and further optimize the noncovalent attractive and repulsive potentials in the framework of the X-Pol method. As a model for the development of a next-generation force field for macromolecular simulations, the accuracy may be further improved by letting parameters depend on atom type and hybridization state—such a parametrization would be used only for nonreactive systems or nonreactive subsystems.

The p orbital exponential parameter for hydrogen used here is $\zeta = 0.88997\ a_0^{-1}$. One may convert this to an equivalent Gaussian exponential parameter α by the STO-1G prescription, which yields[21]

$$\alpha = 0.175967\zeta^2$$

One then obtains $\alpha = 0.13937\ a_0^{-2}$, which compares well to the value $\alpha = 0.141\ a_0^{-2}$ used for the diffuse p orbital in the STO-3G(,P) basis set of paper 1 even though no such correspondence was used in optimizing the parameters of PMOv1.

5. CONCLUDING REMARKS

We have developed a new parametrized semiempirical molecular orbital model that includes polarization effects much more

realistically than previous parametrizations, and we illustrated it for calculations on systems composed of oxygen and hydrogen atoms, such as water clusters and various protonated hydrogen−oxygen compounds.

The difficulty in modeling hydrogen bonding interactions using semiempirical models is well-known, and it has been a continuing challenge since the original MNDO and subsequent AM1 and PM3 methods. Despite many efforts in parametrization in the past 40 years, even with the very recent and carefully parametrized PM6, the ability to describe hydrogen bonding interactions remains the weakest feature in semeimpirical methods and the most difficult to improve. To extend semiempirical methods to model biological systems as a quantal force field, this is the key issue that must be solved. The present papers demonstrated that there is a good theoretical foundation (paper 1) and an excellent practical opportunity (paper 2) to make this happen. We note that no other semiempirical methods predict the water cluster geometries and energies even remotely close to the ab initio results; the present PMO method can yield good results for both the geometries and the energies of these clusters.

The new method is available in a version of MOPAC distributed free of charge on the Internet.[51]

■ ASSOCIATED CONTENT

Supporting Information. Additional structures as in Figure 6 but as obtained with each of the NDDO methods. This material is available free of charge via the Internet at http://pubs.acs.org.

■ AUTHOR INFORMATION

Corresponding Authors
*E-mail: truhlar@umn.edu (D.G.T.), gao@jialigao.org (J.G.).

■ ACKNOWLEDGMENT

This work was supported in part by the National Institutes of Health (grant no. RC1-GM091445) and the National Science Foundation (grant no. CHE09-56776).

■ REFERENCES

(1) Dewar, M. J. S.; Zoebisch, E. G.; Healy, E. F.; Stewart, J. J. P. *J. Am. Chem. Soc.* **1985**, *107*, 3902.
(2) Stewart, J. J. P. *J. Comput. Chem.* **1989**, *10*, 209.
(3) Pople, J. A.; Santry, D. P.; Segal, G. A. *J. Chem. Phys.* **1965**, *43*, S129.
(4) Dewar, M. J. S.; Thiel, W. *J. Am. Chem. Soc.* **1977**, *99*, 4899.
(5) Gao, J. *J. Phys. Chem. B* **1997**, *101*, 657. Xie, W.; Gao, J. *J. Chem. Theory Comput.* **2007**, *3*, 1890.
(6) Xie, W.; Song, L.; Truhlar, D. G.; Gao, J. *J. Chem. Phys.* **2008**, *128*, 234108. Xie, W.; Orozco, M.; Truhlar, D. G.; Gao, J. *J. Chem. Theory Comput.* **2009**, *5*, 459.
(7) Fiedler, L.; Gao, J.; Truhlar, D. G. *J. Chem. Theory Comput.* **2011**, DOI: 10.1021/ct1006373.
(8) Parkinson, W. A.; Zerner, M. C. *J. Chem. Phys.* **1991**, *94*, 478.
(9) Bredow, T.; Jug, K. *Theor. Chem. Acc.* **2005**, *113*, 1.
(10) McNamara, J. P.; Hillier, I. H. *Phys. Chem. Chem. Phys.* **2007**, *9*, 2362.
(11) Morgado, C. A.; McNamara, J. P.; Hillier, I. H.; Burton, N. A.; Vincent, M. A. *J. Chem. Theory Comput.* **2007**, *3*, 1656.
(12) McNamara, J. P.; Sharma, R.; Vincent, M. A.; Hillier, I. H.; Morgado, C. A. *Phys. Chem. Chem. Phys.* **2008**, *10*, 128.
(13) Roothaan, C. C. J. *Rev. Mod. Phys.* **1951**, *23*, 69.
(14) Mitoraj, M. P.; Michalak, A.; Ziegler, T. *J. Chem. Theory Comput.* **2009**, *5*, 962.
(15) Jeziorski, B.; Moszynski, R.; Szalewicz, K. *Chem. Rev.* **1994**, *94*, 1887.
(16) Bickelhaupt, F. M.; Baerends, E. J. *Rev. Comp. Chem.* **1999**, *15*, 1.
(17) Mo, Y.; Gao, J.; Peyerimhoff, S. D. *J. Chem. Phys.* **2000**, *112*, 5530.
(18) Wu, Q.; Yang, W. *J. Chem. Phys.* **2002**, *116*, 515.
(19) Grimme, S. *J. Comput. Chem.* **2004**, *25*, 1463.
(20) Dewar, M. J. S.; Thiel, W. *Theor. Chim. Acta* **1977**, *46*, 89.
(21) Stewart, R. *J. Chem. Phys.* **1970**, *52*, 431.
(22) Dewar, M. J. S.; Low, D. H. *J. Am. Chem. Soc.* **1972**, *94*, 5296.
(23) Repasky, M. P.; Chandrasekhar, J.; Jorgensen, W. L. *J. Comput. Chem.* **2002**, *23*, 1601.
(24) Rocha, G. B.; Freire, R. O.; Simas, A. M.; Stewart, J. J. P. *J. Comput. Chem.* **2006**, *27*, 1101.
(25) Stewart, J. J. P. *J. Mol. Model.* **2007**, *13*, 1173.
(26) Thiel, W.; Voityuk, A. A. *J. Phys. Chem.* **1996**, *100*, 616. Hawkins, G. D.; Cramer, D. J.; Truhlar, D. G. *J. Phys. Chem. B* **1998**, *102*, 3257. Hutter, M. C.; Reimers, J. R.; Hush, N. S. *J. Phys. Chem. B* **1998**, *102*, 8080. Jomoto, L. J.; Nakajima, T. *THEOCHEM* **2002**, *577*, 143. Lopez, X.; York, D. M. *Theor. Chem. Acc.* **2003**, *109*, 149. Dybala-Defratyka, A.; Paneth, P.; Pu, J.; Truhlar, D. G. *J. Phys. Chem. A* **2004**, *108*, 2475. Kwiecień, R. A.; Rostkowski, M.; Dybała-Defratyka, A.; Paneth, P. *J. Inorg. Biochem.* **2004**, *98*, 1078. Nam, K.; Cui, Q.; Gao, J.; York, D. M. *J. Chem. Theory Comput.* **2007**, *3*, 486. Tejero, I.; González-Lafont, .; Lluch, J. M. *J. Comput. Chem.* **2007**, *28*, 997. Sorkin, A.; Truhlar, D. G.; Amin, E. A. *J. Chem. Theory Comput.* **2009**, *5*, 1254.
(27) Pople, J. A.; Head-Gordon, M.; Fox, D. J.; Raghavachari, K.; Curtiss, L. A. *J. Chem. Phys.* **1989**, *90*, 5622.
(28) Martin, J. M. L. *J. Chem. Phys.* **1992**, *97*, 5012.
(29) Page, R. H.; Larkin, R. J.; Shen, Y. R.; Lee, Y. T. *J. Chem. Phys.* **1988**, *88*, 2249.
(30) The H_3O^+ zero point energy was calculated using the MC-QCISD/3 method: Lynch, B. J.; Truhlar, D. G. *J. Phys. Chem. A* **2003**, *107*, 3898. with a scale factor of 0.994, as recommended: Zhao, Y.; Truhlar, D. G. *J. Phys. Chem. A* **2004**, *108*, 6908.
(31) *CRC Handbook of Chemistry and Physics, 2010−2011*, 91st ed.; Haynes, W. M., Ed.; CRC Press: New York, 2010; p 9−24.
(32) *Landolt-Bornstein Zahlenwerte und Funktionen*; Springer: Berlin, 1962; Vol 6, Aufl. Band II/8 S.6, p 871.
(33) Dyke, T. R.; Muenter, J. S. *J. Chem. Phys.* **1973**, *59*, 3125.
(34) Dahlke, E. E.; Orthmeyer, M. A.; Truhlar, D. G. *J. Phys. Chem. B* **2008**, *112*, 2372.
(35) Tschumper, G. S.; Leininger, M. L.; Hoffman, B. C.; Valeev, E. F.; Schaefer, H. F., III; Quack, M. *J. Chem. Phys.* **2002**, *116*, 690.
(36) Bouteiller, Y.; Desfrancois, C.; Abdoul-Carime, H.; Schermann, J. P. *J. Chem. Phys.* **1996**, *105*, 6420.
(37) Kolos, W.; Wolniewicz, L. *J. Chem. Phys.* **1968**, *49*, 404.
(38) Shiner, D.; Gilligan, J. M.; Cook, B. M.; Lichten, W. *Phys. Rev. A* **1993**, *47*, 4042.
(39) Herzberg, G. *Molecular Spectra and Molecular Structure. I. Diatomic Molecules*; Prentice-Hall, Inc.: New York, 1939; pp 487−489.
(40) Neumark, D. M.; Lykke, K. R.; Anderson, T.; Lineberger, W. C. *Phys. Rev. A* **1985**, *32*, 1890.*Landolt-Bornstein Zahlenwerte und Funktionen*; Springer: Berlin, 1962; Vol 6, Aufl. Band II/8 S.6, p 871.
(41) Ruscic, B.; Wagner, A. F.; Harding, L. B.; Asher, R. L.; Feller, D.; Dixon, D. A.; Peterson, K. A.; Song, Y.; Qian, X.; Cheuk-Yiu, N.; Liu, J.; Chen, W.; Schwenke, D. W. *J. Phys. Chem. A* **2002**, *106*, 2727.
(42) Celotta, R. J.; Bennett, R. A.; Hall, J. L. *J. Chem. Phys.* **1974**, *60*, 1740.
(43) Rosenbaum, N. H.; Owrutsky, J. C.; Tack, L. M.; Saykally, R. J. *J. Chem. Phys.* **1986**, *84*, 5308.
(44) Sears, T. J.; Bunker, P. R.; Davies, P. B.; Johnson, S. A.; Spirko, V. *J. Chem. Phys.* **1985**, *83*, 2676.

(45) Polyansky, O. L.; Jensen, P.; Tennyson, J. *J. Chem. Phys.* **1994**, *101*, 7651.
(46) Zhao, Y.; Truhlar, D. G. *Theor. Chem. Acc.* **2008**, *120*, 215.
(47) Lynch, B. J.; Zhao, Y.; Truhlar, D. G. *J. Phys. Chem. A* **2003**, *107*, 1384.
(48) Knizia, G.; Adler, T. B.; Werner, H.-J. *J. Chem. Phys.* **2009**, *130*, 054104.
(49) Kendall, R. A.; Dunning, T. H., Jr.; Harrison, R. J. *J. Chem. Phys.* **1992**, *96*, 6769.
(50) Bryantsev, V. S.; Diallo, M. S.; van Duin, A. C. T.; Goddard, W. A., III. *J. Chem. Theory. Comput.* **2009**, *5*, 1016.
(51) Stewart, J. J. P.; Fiedler, L. J.; Zhang, P.; Zheng, J.; Rossi, I.; Hu, W.-P.; Lynch, G. C.; Liu, Y.-P.; Chuang, Y.-Y.; Pu, J.; Li, J.; Cramer, C. J.; Fast, P. L.; Gao, J.; Truhlar, D. G. *MOPAC*, version 5.017mn (2010); University of Minnesota: Minneapolis and Saint Paul, MN. This program is available at http://comp.chem.umn.edu/mopac (accessed Jan 2011).
(52) Stewart, J. J. P. *J. Comput.-Aided Mol. Des.* **1990**, *4*, 1.
(53) Rybak, S.; Jeziorski, B.; Szalewicz, K. *J. Chem. Phys.* **1991**, *95*, 6576.
(54) Su, P.; Li, H. *J. Chem. Phys.* **2009**, *131*, 14102.
(55) Hunter, E. P.; Lias, S. G. *J. Phys. Chem. Ref. Data* **1998**, *27*, 413.
(56) *CRC Handbook of Chemistry and Physics*, 80th ed.; Lide, D. R., Ed.; CRC Press, Inc.: New York, 1999; pp 10−175.
(57) Karton, A.; Parthiban, S.; Martin, J. M. L. *J. Phys. Chem. A* **2009**, *113*, 4802.
(58) Ng, C. Y.; Trevor, D. J.; Tiedemann, P. W.; Ceyer, S. T.; Kronebusch, P. L.; Mahan, B. H.; Lee, Y. T. *J. Chem. Phys.* **1977**, *67*, 4235.
(59) Harder, E.; Anisimov, V. M.; Vorobyov, I. V.; Lopes, P. E. M.; Noskov, S. Y.; MacKerell, A. D., Jr.; Roux, B. *J. Chem. Theory Comput.* **2006**, *2*, 1587.
(60) Harder, E.; Anisimov, V. M.; Whitfield, T.; MacKerell, A. D., Jr.; Roux, B. *J. Phys. Chem. B* **2008**, *112*, 3509.
(61) Gao, J.; Habibollazadeh, D.; Shao, L. *J. Phys. Chem.* **1995**, *99*, 16460.
(62) Gao, J. *J. Comput. Chem.* **1997**, *18*, 1062.
(63) Xie, W.; Pu, J.; Mackerell, A. D., Jr.; Gao, J. *J. Chem. Theory Comput.* **2007**, *3*, 1878.
(64) Xie, W.; Pu, J.; Gao, J. *J. Phys. Chem.* **2009**, *113*, 2109.
(65) Voityuk, A. A.; Rösch, N. *J. Phys. Chem. A* **2000**, *104*, 4089.
(66) Tang, K. T.; Toennies, J. P. *J. Chem. Phys.* **1984**, *80*, 3726.
(67) Misquitta, A.; Stone, A. *Mol. Phys.* **2008**, *106*, 1631.
(68) Grimme, S.; Antony, J.; Ehrlich, S.; Krieg, H. *J. Chem. Phys.* **2010**, *132*, 154104.